Electrochemical Water Splitting Using NiO-$NiFe_2O_4$/MWCNTs Nanocomposite as Electrocatalyst

[1]Rida Noor, [2*]Muhammad Shahid, [3]Fahd Nawaz Khan, [4]Malik Adeel Umer

[1,2,4]School of Chemical & Materials Engineering,
National University of Sciences & Technology, H-12, Islamabad, Pakistan
[3]Faculty of Materials and Chemical Engineering,
Ghulam Ishaq Khan Institute of Engineering Sciences and Technology,
Topi, Swabi, Pakistan
[1]ridabukhari410@gmail.com, [2*]mshahid@scme.nust.edu.pk, [3]fahd@giki.edu.pk, [4]umer.adeel@scme.nust.edu.pk

Received: August 31 2021, Accepted: January 26, 2022 Published: January 31, 2022

Abstract

Escalating energy demands, scarcity of conventional energy resources and environmental concerns are the key to fuel production through water splitting. Various electrocatalysts have been reported, considering the cost effectiveness, stability and OER (oxygen evolution reaction) activity. In the same context, porous hybrid NiO-$NiFe_2O_4$/MWCNTs based nanocomposite as an OER electrocatalyst, has been investigated in the current study. The synthesis has been accomplished via co-precipitation using Tween as a surfactant. Characterization and electrochemical study for water electrolysis using synthesized electrocatalyst deposited glassy Carbon (GC) electrode as anode was carried out using relevant tools. Iron-doped Nickel oxide nanoparticles were synthesized recognizing excellent oxygen evolution activity of NiO and its increase in conductivity with Fe incorporation due to its higher electropositivity. Nanocomposites were synthesized by incorporating upto 20% weight percent MWCNT (Multiwall carbon nanotubes). High surface to volume ratios, stability and excellent conductivity of MWCNTs furthermore, reduction of crystallite sized due to their incorporation enhanced the performance of the electrocatalyst significantly. Hybrid formation of NiO and $NiFe_2O_4$ at a certain calcination temperature was also found to be the reason for enhanced OER activity due to the increased grain boundaries. Porous NiO-$NiFe_2O_4$/MWCNTs with 10% MWCNTs concentration outperformed with 35mA/cm^2 of current density at 1.8V in alkaline media.

Keywords: $NiFe_2O_4$, NiO, f-MWCNTs, Electrocatalyst, Energy, OER, water splitting.

Introduction

Energy plays an essential role in the economy of any nation, however, increasing environmental concerns demand further to search for renewable and clean energy resources. Fuel production through water splitting has been considered as one of the dependable sources to meet such concerns. Water is abundant and a clean source of hydrogen generation. Hydrogen due to its light weight, high energy density, high storage capabilities and environmental friendliness, is considered a promising fuel. During water splitting reaction hydrogen evolution is relatively easy, however, oxygen evolution requires manipulation with anode catalyst to obtain relatively lower activation potential.

As OER (Oxygen evolution reaction) occurs in multiple steps requiring electrons in each step hence they have got a wide activation potential barrier. The slow OER is due to high activation energy for the transfer of electrons and, therefore, search for an efficient OER catalyst is of high interest [1].

Metal oxides are considered as one of the most important candidates of WOCs (Water oxidation catalysts) family due to their higher electrical conductivity, atomic diffusivity, oxygen ion mobility and catalytic activity. Their high catalytic activity is attributed to the presence of different kinds of defects including vacant lattice sides, electron-hole pairs, interstitials sites, dislocations and impurity etc. [2-3]. Ir, Ru, IrO_2 and RuO_2 have been considered the best known catalysts for both acidic and basic media.[4-5] However, their industrial application for water electrolysis is limited due to their scarcity and high costs [6]. $IrO_x/SrIrO_3$, Cu_2O, Cu_2O/ITO, Ir_xO/ATO and TiO_2/CuO have also been studied widely [7-9]. Some metallic catalysts have been found to form stable oxide layers, thereby, showing good electrolytic activities, however, all metallic catalysts are not considered suitable. For example, Ru when is used in metallic form rather than its oxide form, shows significant OER, however, oxide layer formed on its surface is unstable and dissolving during reaction [10]. $CoFe_2O_3$, $NiCo_2O_4$, $MnCo_2O_4$, $CuCo_2O_4$ and $ZnCoO_4$ are some of the other noticeably good electro-catalysts. The reason for their good performance has been attributed to the non-uniform charge distribution, thereby, generating active sites. High conductivity is also desirable along with active sites which can be achieved by doping with high conductivity metals [11-13]. Intrinsic conductivity of active metals (e.g Ni, Fe, Mn, Co etc.) makes them attractive candidates for OER. They usually form oxide layers on their surface during OER mechanism. One of the pitfalls of spontaneous formation of oxide layer on their surface is uncontrolled composition of their lattice structure but still their fresh growth is advantageous for aging issues [14]. Ni having oxidation state +2 (in NiO) which is compatible with the oxidation state for OER and is considered the most active catalyst, however, has relatively inferior crystallinity; it can be improved by incorporation of conductive metals [15]. Although smaller particle size leads to greater surface area resulting in improved activity, however, crystallinity and conductivity are compromised. Therefore, for the optimization of activity and conductivity simultaneously, incorporation of Fe, Mo and Co have been proved to be better for electrolysis compared with pure NiO and its alloys. However, iron has demonstrated higher efficiency [16]. Fominykh et al [17] reported the synthesis of $Fe_xNi_{1-x}O$ nanoparticles with doping concentration of Fe up to 20% and observed decrease in particle size with increasing concentration of iron. 10% Fe doped particles showed superior OER efficiency and turn over frequency even higher than IrO catalyst in basic media. Similarly, Trotochaud et al [18] reported a study of intentional and unintentional electrochemical incorporation of Fe in Nickel hydroxide and oxy-hydroxide films; Fe inclusion showed almost 30-fold improved activity in basic media. Fe incorporation is believed to provide abundance of Ni^{+3}/Ni^{+4} and Ni vacancies due to its higher electronegativity resulting in increased efficiency [19-

https://doi.org/10.24949/njes.v14i2.660

20]. Zhang et al reported the fabrication of Ni/NiO on a carbon fiber paper, with good stability in basic media.[21] Louie et al also reported Ni, Fe and Fe-Ni based electro-catalytic films fabricated via electro-deposition over gold electrodes. Ni-Fe films with 40% of iron content showed 3 and 2 folds higher OER efficiency comparing to pure Fe and Ni films, respectively [22]. Song et al reported synthesis of Iron-Nickel electro-catalyst and claimed the outperformance of the synthesized catalyst over all the other existing reported Iron-Nickel oxide catalysts. Catalyst was electrochemically deposited over Ni Foam, Au and GC (Glassy Carbon) substrates for comparison; all substrates types showed near equal performance [23].

Carbon based compounds also have been studied for electrolysis. Although due to highly ordered lattice sp^2 hybrid structures, OER overpotentials of carbons are significantly higher, however, their low costs, good conductivity, high surface area and design versatility makes them attractive for electro-catalytic applications [24-25]. Greater activation sites are required for better OER; it can be generated by manipulating hexagonal sp^2 network by functionalization, for example, by acid treatment [26-27]. Gong et al reported the synthesis of Ni/NiO nano-composite with CNTs via hydrolysis. Ni/CNT, NiO/CNT and CNT alone showed inferior HER performance compared with NiO/Ni-CNT composite. Outperformance of NiO/Ni-CNT composite is credited to its higher surface area and collaboration of NiO and Ni [28].

NiO and Fe-doped Nickel oxides have been considered excellent and most suitable candidates as electrocatalysts for electrochemical water splitting. Although incorporation of CNTs in Nickel oxides has been reported, however, porous NiO-$NiFe_2O_4$ hybrid with MWCNTs has not been well-attempted. This paper discusses a facile composition of porous hybrid NiO-$NiFe_2O_4$/MWCNTs electrocatalyst for electrochemical water splitting in alkaline media; the electrocatalyst has been found suitable for mass production along with its low cost and stability.

Experimentation

Chemicals

$Ni(NO_3)_2.6H_2O$ (> 99.0%, Sigma Aldrich), $Fe(NO_3)_3.9H_2O$ (>99.0%, Sigma Aldrich), acetone (> 99.8%, VWR Chemicals), ethanol (> 99.9%, Labscan Asia Co. Ltd), MWCNTs (> 90%, Sun Nanotek Co. Ltd.), Tween 85 (Sigma Aldrich), Nafion (Sigma Aldrich).

Synthesis of $NiFe_2O_4$ Nanoparticles without Tween

Iron Nickel Oxide nanoparticles were synthesized by co-precipitation method. Iron to Nickel ratio was kept as 15:85. Solution of 1M NaOH in 50ml deionized water was prepared by pouring 2mg of NaOH in 50ml of DI (deionized) water, under stirring at a temperature of 60ºC and was named as Solution-1. Another 2.5M solution of $Fe(NO_3)_3.9H_2O$ and $Ni(NO_3)_2.6H_2O$ in 20ml of DI water was prepared by adding 3mg and 12.35mg of iron nitrate and nickel nitrate, respectively; this solution designated as Solution-2, was stirred well enough for 1 hour. Afterwards, Solution-2 was drop-wise added in Solution-1 maintained at 60ºC; the stirring continued for 4 hours at the same temperature. Later, washing was done by centrifugation at 3500rpm for 15min at ambient temperature. Sample was thoroughly washed two times with DI water, one time with acetone and again twice with DI water. The collected samples were dried at 60ºC overnight in oven and later were calcinated at different temperatures (between 500ºC and 800ºC) for 3hrs in a muffle furnace, for comparison.

Synthesis of $NiFe_2O_4$ Nanoparticles with Tween

Iron Nickel Oxide NPs (nanoparticles) were prepared by the same procedure as discussed in the previous section, however, with the addition of surfactant (Tween85). 10ml of the Tween was added in 1M NaOH solution in 50ml DI water at 60ºC with vigorous stirring. Solution-2 was prepared in the same manner and after drop wise addition in Solution-1 maintained at 60ºC in oven for 4 hrs. Afterwards, washing via centrifugation, drying and calcination at different temperatures were also performed as per previously mentioned scheme.

Functionalization of MWCNTS

MWCNTs were functionalized using acidic approach. 0.65g of the CNTs were added into 15ml mixture of concentrated acid HNO_3/H_2SO_4 (1/3 v/v) and was sonicated for half an hour. In an oil bath with temperature of 90ºC, the dispersed mixture was suspended and was refluxed for 7.5 hours under continuous stirring. Acid treatment was used for introducing eCOOH on the walls of MWCNTs, which was expected not only to enhance chemical reactivity but also to remove residual impurities [29]. Elimination of residual impurities resulted in reduction of charge carrier inhomogeneity leading to better charge mobility thereby enhancing electrochemical properties of the catalyst. Neutralization of the MWCNTs was then performed by centrifugation several times with DI water until neutral pH was obtained, followed by drying at 70ºC in a vacuum oven.

Formation of NiO-$NiFe_2O_4$/ functionalized MWCNTs Nanocomposites

Composites of synthesized Nickel iron oxide NPs (both with and without surfactant) with various proportions of functionalized CNTs (5%, 10%, 15% and 20%) were prepared by making dispersion in orthoxylene. For each composite NPs and MWCNTs were both poured separately in specific proportions in 10ml orthoxylene and sonicated (SONREX Digit DT52 H, BANDELIN, Germany 240 Watts, 35kH) for 1.5hr. Afterwards these were mixed dropwise and sonicated at ambient temperature for 16 hours for thorough dispersion, followed by drying at 60ºC overnight in oven and grinding using mortar & pestle for more than an hour, resulting into nanocomposites. The same procedure was followed for fabrication of all composites using mentioned proportions of the ingredients.

Preparation of Anode

For preparation of an anode 2 mg of the sample was poured into 1 ml solution of DI water and ethanol in a ratio of 2:1, respectively. For 2:1 solution of DI: ethanol, 320 µl of the ethanol was poured into 680µl of deionized water (DI). 30µl of Nafion was also poured as a binder. The solution was then sonicated for 1hr in a bath sonicator. With the help of micropipette 5µl of the mixture was then drop-cast on a cleaned GC (glassy Carbon) electrode. The electrode was then left overnight for drying at ambient temperature.

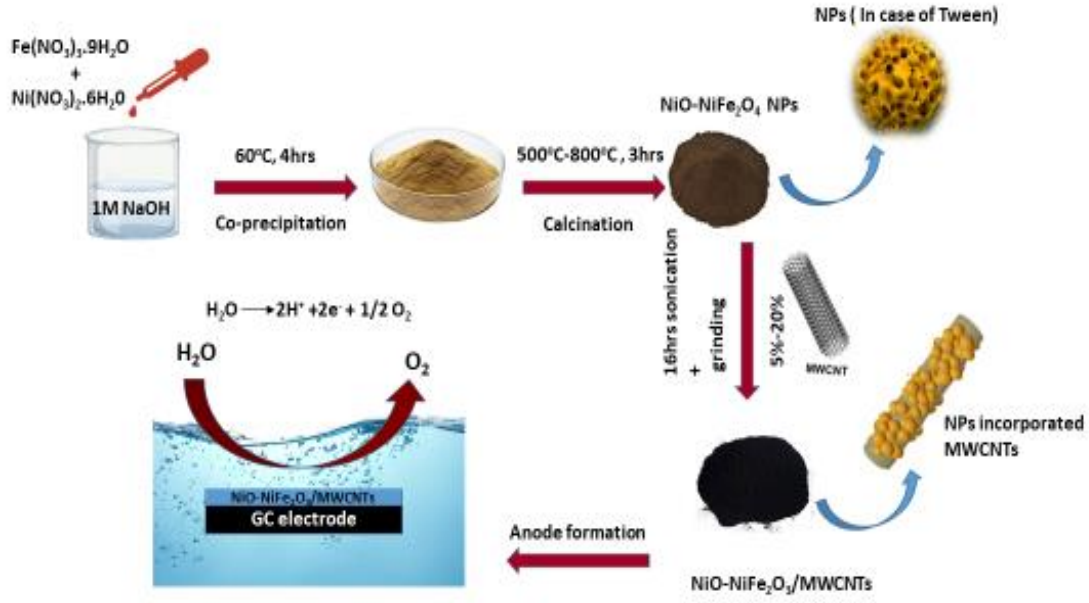

Figure 2: Schematic diagram of NiO-NiFe2O4/ f-MWCNT synthesis

Results and Discussion

Structure confirmation and investigation of crystallographic properties of the synthesized catalysts was conducted by XRD (STOE-Seifert X'pert PRO), using CuKα radiations (λ=0.154 nm). Fig.2(a) exhibits XRD graph of the NiO-$NiFe_2O_4$ Nanoparticles synthesized without surfactant, calcinated at various temperatures for 3hrs. Absence of well-defined peaks for particles calcinated below 600ºC, depicted that the formation of the phase started at 600ºC and below this temperature the structure was amorphous with no crystalline phase.

Diffraction peaks at 2θ= 18º (111), 30º (220), 35.4º (311), 37º (222), 43º (400), 53.5º (422), 57º (511), 62.7º (440), 70.7º (620), 73.9º (533) and 79º (444) confirmed the formation of cubic structure of $NiFe_2O_4$ with JCPDS Card No.01-088-0380. Whereas peaks around 37º (111), 43º (200), 62.7º (220) and 79º (222) confirms the formation of NiO phase with JCPDS Card No 847-1049. No extra peaks were obtained depicting the absence of any significant amount of any kind of impurity. Furthermore, it was observed that the peak intensity was increased with increasing temperature from bottom to top, whereas, and the width decreased; this could be attributed to the increasing crystallite size with increase in temperature [30]. Another factor to be considered here was that at 800ºC NiO phase (which is more dominant at 700ºC) had vanished.

This might also have contributed to the increase of crystallite size, since hybrids and doping had been acknowledged to cause reduction of crystallite size [31-33].

Fig. 2(b) exhibits the XRD graph of Nickel Iron Oxide synthesized using a surfactant (Tween); peaks at 2θ= 18º (111), 30º (220), 35.4º (311), 37º (222), 43º (400), 53.5º (422), 57º (511), 62.7º (440), 70.7º (620), 73.9º (533) and 79º (444) were recognized. The obtained peaks with specified hkl planes assured the formation of cubic structure of $NiFe_2O_4$ (JCPDS Card no.01-088-0380).

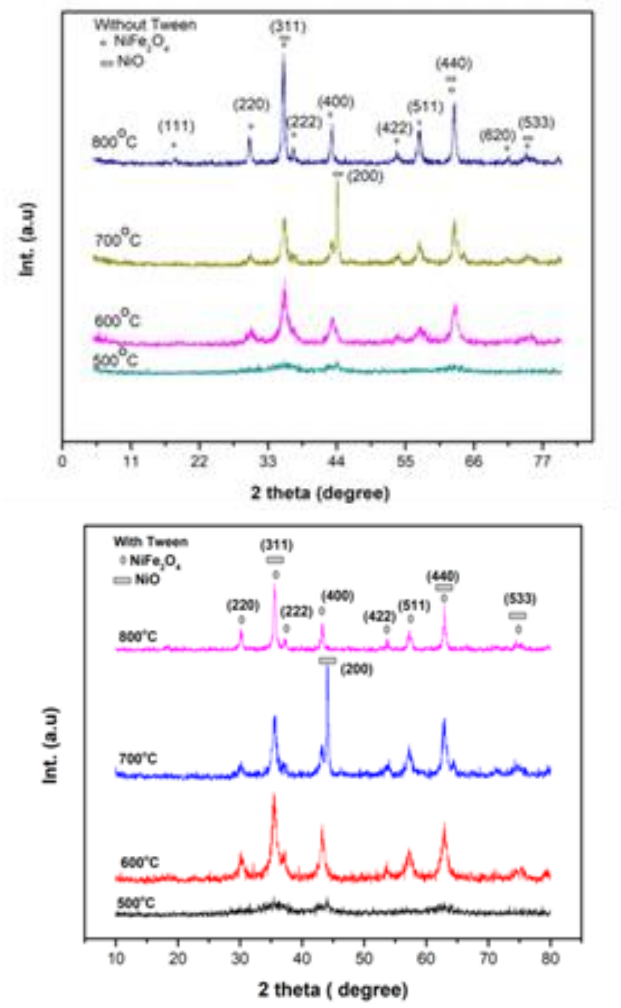

Figure 2: (a) XRD patterns of NiFe2O4 (a) synthesized without Tween (b) synthesized with Tween

Neither extra peaks were found nor any peak shift was observed, indicating the absence of any significant impurity. Whereas peaks around 37º (111), 43º (200), 62.7º (220) and 79º (222) confirmed the formation of NiO phase with JCPDS Card no 847-1049. Like NPs without surfactant, the peak intensity and width for NPs with surfactant followed a similar trend and exhibited no NiO peak at 800ºC. The XRD patterns for the both cases (i.e. with and without Tween) appeared similar.

Fig.3 manifests a comparison of XRD patterns of pure NiO-$NiFe_2O_4$ and NiO-$NiFe_2O_4$/ MWCNTs (various percentages). Diffraction peaks at 2θ= 18º (111), 30º (220), 35.4º (311), 37º (222), 43º (400), 53.5º (422), 57º (511), 62.7º (440), 70.7º (620), 73.9º (533) and 79º (444) were obtained for pure NiO-$NiFe_2O_4$ and NiO-$NiFe_2O_4$ /MWCNTs composite. Only a small negligible peak was obtained at around 26º which could be attributed to uniform distribution and anchoring of NiO-$NiFe_2O_4$ on CNTs. Another reason for this small peak could be attributed to the very small quantity of CNTs in comparison to NiO-$NiFe_2O_4$ [34]. Also a small change in the FWHM (full width at half maximum) was observed. CNTs incorporation slightly increased FWHM which could be attributed to the introduction of impurity due to CNTs and reduction of crystallite size.[35] This comparison also indicated that no phase change occurred in case of formation of CNTs composite.

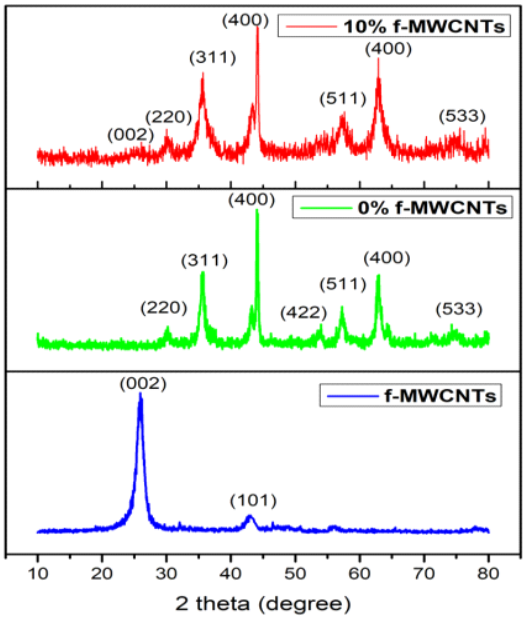

Figure. 3: Comparison of pure NiO-$NiFe_2O_4$ and NiO-$NiFe_2O_4$ / f-MWCNTs (10%)

Crystallite sizes of the samples were calculated using Debye Scherrer formula. The Tables 1-2 clearly indicate variation of the crystallite sizes with varying parameters. Three major parameters are essential to be considered here. First, samples prepared in the presence of surfactant (Tween 85) showed smaller crystallite sizes compared with samples without surfactant. The smaller crystallite sizes in the presence of surfactant could be attributed to the amphiphilic nature of surfactant which controlled the size of nanoparticle by capping. Capping reduced surface energy resulting in controlled growth [36]. Another trend that noticed in the Table 1, was that increasing calcination temperature increased crystallite size due to Ostwald ripening, which was also prominent by XRD patterns; at higher temperatures the peaks were sharper, showing more crystallinity and an increase in crystallite size [37]. Thirdly, incorporation of MWCNTs reduced the crystallite sizes from 18.47nm to 14.28nm for 10% MWCNTs incorporation, which could be attributed to the fact that introduction of MWCNTs cut the grains by creating networks within and outside the grain boundaries.

Table-1. Variation of crystallite size with calcination temperatures.

Calcination Temperature	600ºC	700ºC	800ºC
Crystallite Size (nm)	18.21	20.8	45.48
Crystallite Size (nm) with Tween	13.82	18.47	31.6

Table-2. Variation of crystallite size with MWCNTs concentration.

MWCNTs Percentage	0%	10%	20%
Crystallite Size (nm)	18.47	14.28	11.37

Nitrogen sorption was performed at 77ºK with dried powders after degassing of Iron Nickel Oxide NPs and Iron Nickel Oxide/MWCNTs nanocomposites at 150ºC for 12 hours. BET analysis of the nanoparticles synthesized with and without surfactant showed a significant difference in their surface areas and pore sizes. Tables 3 & 4 and Fig. 4 illustrate the BET results.

Table 3: Surface areas and porosities of the synthesized adsorbents
(T represents samples prepared with Tween whereas WT represents samples prepared without Tween)

Adsorbent	T600^{O}C	T700^{O}C	T800^{O}C	WT800^{O}C
BET surface area (m^2/g)	50.95	23.06	18.37	13.86
Pore size (nm)	35.75	76.61	124.49	17.43

Table 4: Surface areas and porosities of composite adsorbents.

Adsorbent	MWCNTs	0%	10%	20%
BET surface area (m^2/g)	68.18	23.06	77.47	70.47
Pore size (nm)	42.88	76.61	63.7	12.36

Fig.4(a) shows the BET analysis trend of surface area with increasing temperature in the case of sample prepared in the presence of surfactant (Tween). The decreasing surface area with increasing temperature can be attributed to the fact that an increase in temperature increases crystallite size and reduces surface area [38]. Fig.4(b) shows the increase of pore size with increase in temperature; the pore size is, presumably, increased due to the removal of surfactant.

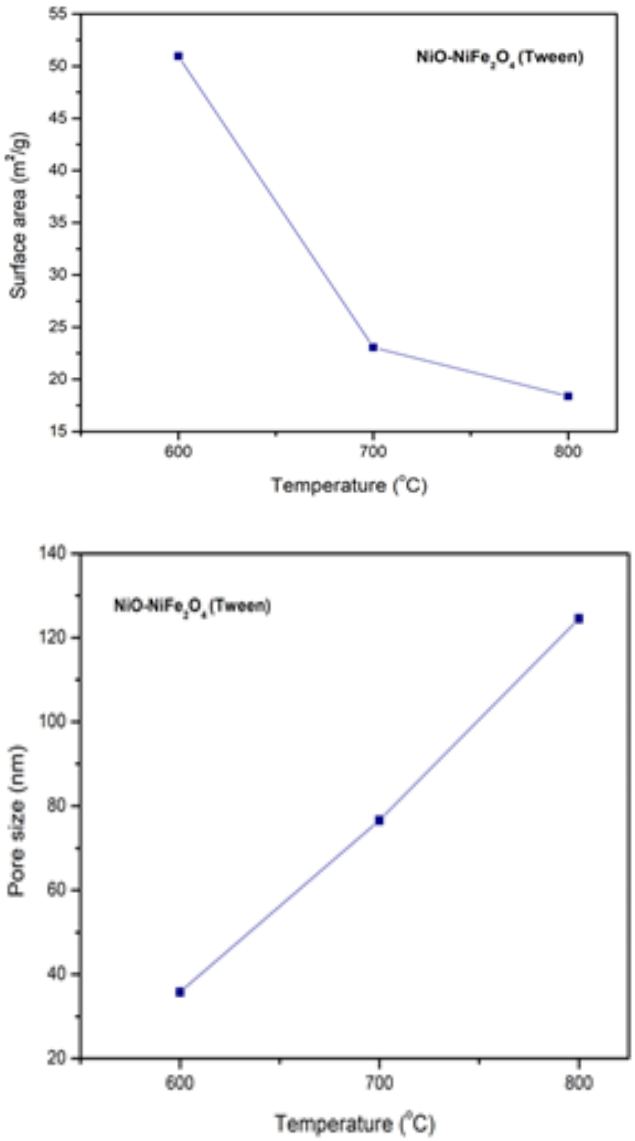

Figure.4: Effect of temperature on (a) surface area and (b) pore size of NiO-NiFe2O4 (Tween).

Fig.5 shows the SEM images of (a) NiO-$NiFe_2O_4$ nanoparticles prepared using surfactant and calcined at 700°C, and (2) the pristine MWCNTs. The pristine MWCNTs were functionalized before incorporating with the nanoparticles to fabricate a nanocomposite, however, no distortion of the MWCNTs structure was observed after acid treatment which was performed for functionalization.

In Fig.6, an SEM image of NiO-$NiFe_2O_4$/f-MWCNTs nanocomposites with 10% MWCNTs concentration is shown. It is evident that the nanoparticles were dispersed/decorated onto CNTs uniformly without any significant agglomeration which can be attributed to strong electrostatic interaction of eCOOH functional group as a result of acidic functionalization [28]. A minute agglomeration formed could be attributed to the extreme magnetic nature of Nickel Iron oxide nanoparticles. Generally, poor sonication can also be a significant factor for non-uniform dispersion, however, that did not seem to be a major reason in this case as sonication was performed for more than 16hrs.

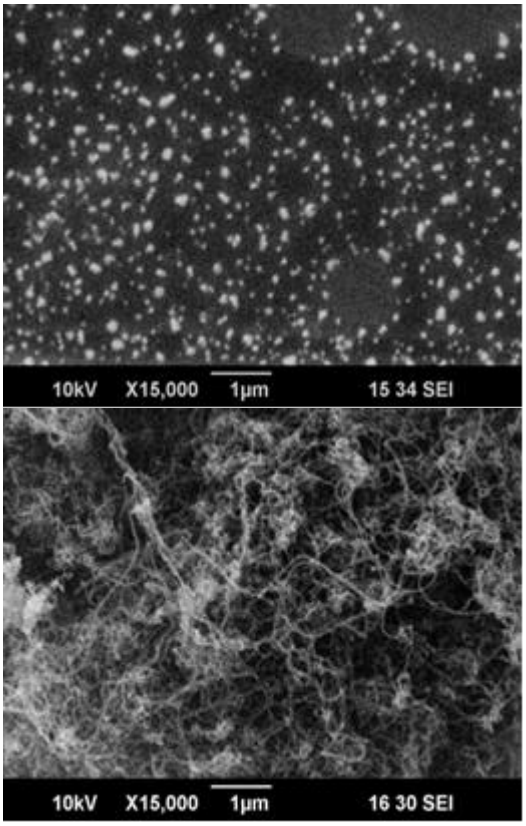

Figure.5: SEM micrographs of (a) NiO-NiFe2O4 nanoparticles synthesized using surfactants at 700oC; (b) pristine MWCNTs.

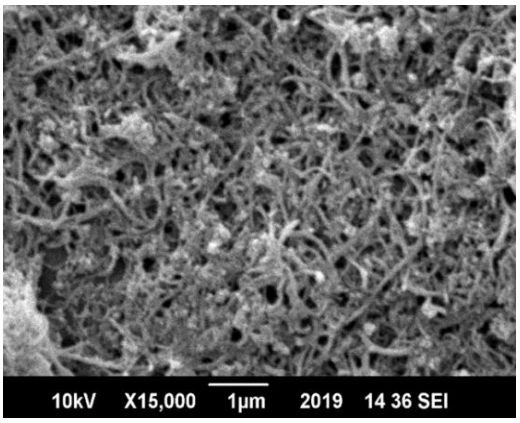

Figure.6: SEM image of NiO-$NiFe_2O_4$/f-MWCNTs nanocomposite with 10% f-MWCNTs.

To confirm the functionalization of MWCNTs, contact angle measurement was carried out. Pristine and functionalized CNTs were dispersed in DI water and drop-cast on cleaned glass slides to form coating. Later contact angle measurement was performed by using Kruss Power drop analyzer. From the Fig. 7(a-b) the difference of contact angles for both is evident.

Pristine CNTs are hydrophobic so, they have large angles, whereas, the functionalized CNTs become hydrophilic and their contact angles are significantly smaller [39]. Dispersibility test of functionalized and pristine CNTs was performed by making dispersion of both types of CNTs in DI water by sonication for

15min and then leaving for a prolonged time. Functionalized CNTs exhibited hydrophilicity uniform dispersion, as is shown in Fig. 7(c). This hydrophilicity can be attributed to the generation of polar groups at the surface of CNTs as a result of acid treatment functionalization [40].

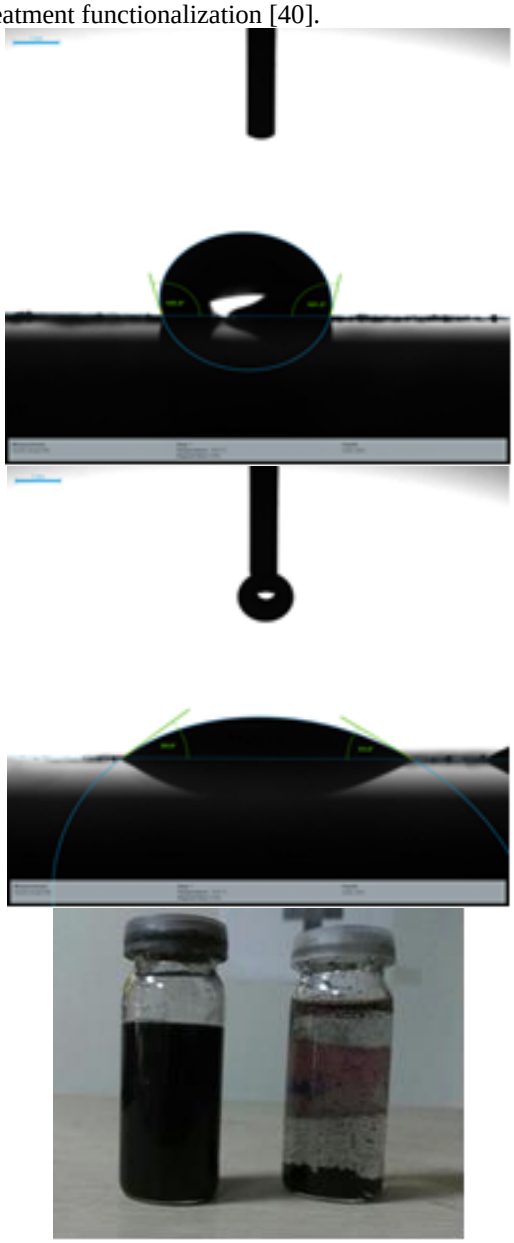

Figure 7: (a) Contact angle of (a) pristine CNTs (b) functionalized CNTs; (c) dispersion of functionalized and pristine CNTs at left and right, respectively

Electrochemical testing was performed by Gamry® framework for electrochemical workstation. Fig.8 displays cyclic voltammetry (CV) performed for this purpose over a potential window of 0.5V to 1.8V. Three-electrode system was used for current measurement as a result of varying voltage. Synthesized electro-catalyst deposited over GC (glassy carbon) electrode was used as working electrode. Whereas, Platinum (Pt) and silver-silver chloride (Ag/AgCl) were used as counter and reference electrodes, respectively. 0.1M KOH solution was used as electrolyte in which all the three electrodes were dipped. For comparison CVs of all the samples (including samples with and without surfactant, calcinated at various temperatures, and their composites with functionalized MWCNTs at various concentrations) were performed at various scan rates. Cyclic voltammetry of the Iron Nickel Oxide NPs synthesized in the presence of the surfactant (Tween 85) were performed for comparison of the prepared samples at various calcination temperatures (600ºC, 700ºC and 800ºC), as shown in Fig.8(b). As I-V curves depict that the sample calcinated at 700ºC outperformed the other two samples calcinated at 600ºC, 700 ºC and 800ºC. Samples calcinated at 600ºC, 700ºC and 800ºC showed 10.5mA/cm^2, 15mA/cm^2 and 8mA/cm^2 of current densities, respectively. The obtained CV results were also supported by XRD and BET results, as shown in Fig.1. At 700ºC a prominent hybrid phase of NiO-$NiFe_2O_4$ was formed as could be seen by XRD graph which showed a prominent peak of NiO at 700ºC. This more prominent NiO phase in NiO-$NiFe_2O_4$ was, presumably, a reason for its outperformance. NiO was believed to be more efficient and active OER catalyst in NiO-$NiFe_2O_4$ hybrid whereas Fe was introduced to increase conductivity [41]. Another factor which could be considered regarding hybrid phase formation was that hybrids were believed to be more active compared with single phase because of their increased grain boundaries resulting in improved activity [42]. On the other hand, it can be seen that sample at 600ºC showed better CV behavior than samples at 800ºC (Fig.8(b)); at higher temperature the crystallite size was increased thereby decreasing surface area and reducing its activity. So, the sample at 600ºC showed better behavior due to its smaller crystallite size (comparing to 800ºC with higher crystallite size). Like the previous case, CVs of porous samples prepared in the presence of surfactant at different temperatures were performed for comparison. Like the comparison for samples without surfactant (Fig.8(a)), I-V curves of porous samples (with surfactant as shown in Fig.8(b)) exhibited higher current densities comparing to the non-porous samples (without surfactant).

Samples calcinated at 600ºC, 700ºC and 800ºC showed 16mA/cm^2, 19mA/cm^2 and 14mA/cm^2 of current densities, respectively. Various CV graphs shown in Fig.8, are well-supported by the XRD (Fig.2) and BET (Tables 1 to 2) analyses. The higher current densities at 700ºC can be attributed to the formation of NiO-$NiFe_2O_4$ at this temperature which can also be confirmed by the corresponding XRD graphs, identical to the previous case. Another factor to be observed is that samples synthesized in the presence of surfactant showed better performances which also can be supported by the BET and XRD analyses; samples prepared in the presence of Tween had lower crystallite sizes and pores leading to better activity and performances comparing to the samples in the absence of surfactant.

The sample synthesized with surfactant and calcinated at 700ºC outperformed and therefore was chosen for the formation of their composites with functionalized MWCNTs. As exhibited by the I-V curve of Fig. 8(c) the samples with 5%, 10%, 15% and 20% showed 25A/cm^2, 35mA/cm^2, 22mA/cm^2 and 20mA/cm^2 of current densities, respectively. Initially, the current density of the nanocomposites increased for 5wt.% and

10wt.% f-MWCNTs due to the high surface to volume ratio of CNTs and hence greater activity.

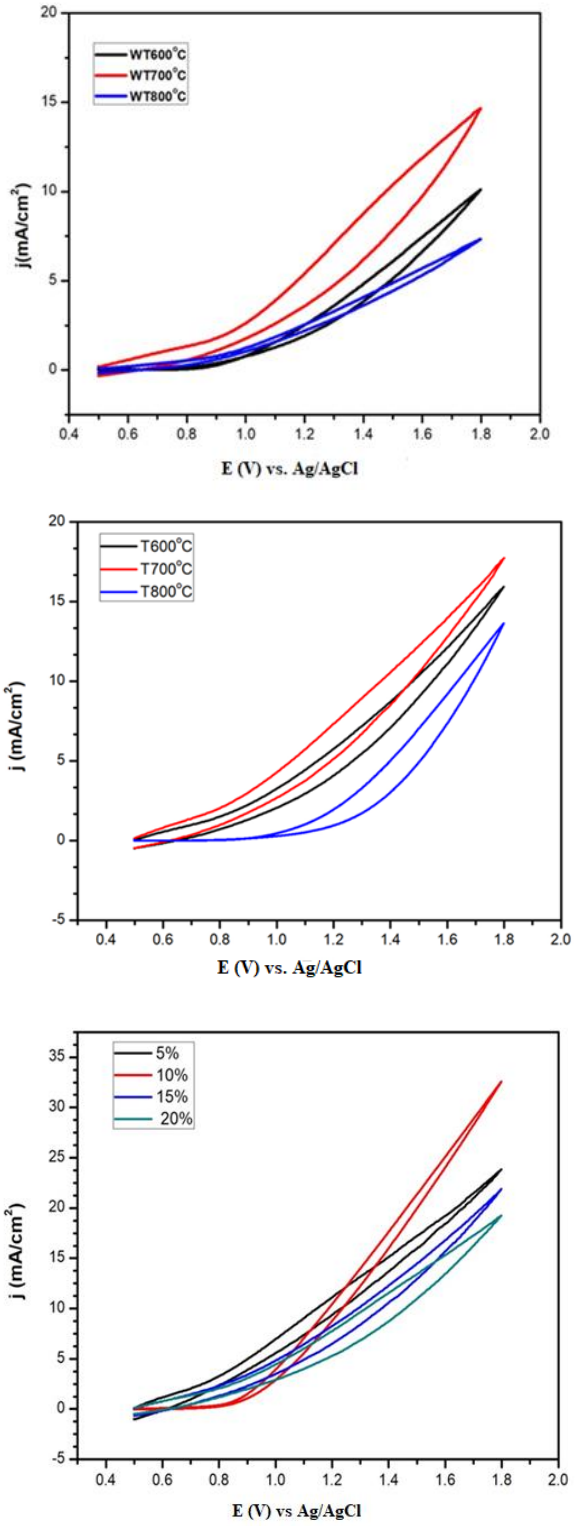

Figure.8: CV curves for NPs synthesized at three different temperatures for NiO-$NiFe_2O_4$ (a) without Tween and (b) with Tween; (c) CV curves for NiO-$NiFe_2O_4$/f-MWCNTs composites synthesized at 700°C with four different CNTs concentrations

However, at higher concentrations 15wt.% and 20wt.% CNTs, the efficiency was decreased, presumably, due to the decrease in the concentration of NiO-$NiFe_2O_4$, which was the core catalyst and was responsible for OER (oxygen evolution reaction).

Conclusions

NiO-$NiFe_2O_4$/MWCNTs nanocomposites were synthesized, with and without surfactant by co-precipitation method. Electrochemical studies were then carried out for water splitting by using electrode, fabricated using synthesized nanocomposites. NiO-$NiFe_2O_4$ hybrid phase of NPs formed under calcination at 700°C, in the presence of surfactant, proved to be superior to the other synthesized NPs and hence were selected for composites formation. Composite with optimized 10% weight fraction of MWCNTs outperformed with current density of 35mA/cm^2 at 1.8V. The presented results proved, fabricated NiO-$NiFe_2O_4$/MWCNTs nanocomposites a promising electro-catalyst for water electrolysis.

REFERENCES:

[1]. Joshua, N.S.L., Spurgeon, M., "Proton exchange membrane electrolysis sustained by water vapor," *Energy Environ. Sci.*, 2011, vol.4, no.8, pp. 2993-2998.

[2]. Wang, Z., Wang, L., "Photoelectrode for water splitting : Materials, fabrication and characterization," Science China Materials, 2018, vol. 61, no. 6, pp. 806–821.

[3]. Dau, H., Limberg, C., Reier, T., Risch, M., Roggan, S., "The Mechanism of Water Oxidation : From Electrolysis via Homogeneous to Biological Catalysis", *ChemCatChem*, 2010, no.2, pp. 724–761.

[4]. Reier, T., Oezasalan, M., Strasser, P., "Electrochatalytic Oxygen Evolution Reaction (OER) on Ru, Ir and Pt Catalysts: A comparative study of Nanoparticles and BulK Materials", ACS Catalysis, 2012, vol. 2, no. 8, pp. 1765-1772.

[5]. Lee, Y., Suntivich, J., May, K., Perry, E., Horn, Y., "Synthesis and Activities of Rutile IrO_2 and RuO_2 Nanoparticles for Oxygen Evolution in Acid and Alkaline Solutions", J. Phys. Chem. Lett, 2012, vol. 3, no. 3, pp. 399-404.

[6]. Jacques, C.V., "Heterogeneous Catalysis on Metal Oxides," *Catalysts*, 2017, vol.7, no.11, pp.341.

[7]. Walter, M.G., Warren, E. L., McKone, J.R., Boettcher, S.W., Mi, Q., Santori, E.A., Lewis, N.S., "Solar Water Splitting Cells", *Chem. Rev*., 2010, vol.110, no.11, pp. 6446–6473.

[8]. Seitz, L., Dickens, C., Nishio, K., Hikita, Y., Montoya, J., Doyle. A., Kirk, C., Vojvodic, A. Hwang, H., Norskov, J., Jaramillo, T., "A highly active and stable $IrO_x/SrIrO_3$ catalyst for the oxygen evolution reaction", Science, 2016, vol. 353, no. 6303, pp. 1011-1014.

[9]. Bandara, J., Udawatta, C.P.K, Rajapakse, C.S.K, " Highly stable CuO incorporated TiO_2 catalyst for photocatalytic hydrogen production from H_2O",

Photochemical and Biological Sciences, 2005, vol. 4, pp. 857-861.

[10]. Mavrokefalos, C.K., Patzke G. R., "Water Oxidation Catalysts : The Quest for New Oxide-Based Materials," Inorganics, 2019, Vol. 7, No. 3.

[11]. Xia, W., Li, N., Li, Q., Ye, K., Xu, C., "Au-$NiCo_2O_4$ supported on three-dimensional hierarchical porous graphene-like material for highly effective oxygen evolution reaction," *Scientific Reports*, 2016, 6:23398, pp. 1–9.

[12]. Liu, X., Cui, S., Sun, Z., Ren, Y., Zhang, X., Du, P., "Self-Supported Copper Oxide Electrocatalyst for Water Oxidation at Low Overpotential and Confirmation of Its Robustness by CuK-Edge X-ray Absorption Spectroscopy," 2016, vol. 120, no. 2, pp. 831-840.

[13]. Kuo, C., Li, W., Pahalagedara, L., El-Sawy, A. M., Kriz, D., Genz, N., Guild, C., Ressler, T., Suib, S. L., He, J., "Understanding the Role of Gold Nanoparticles in Enhancing the Catalytic Activity of Manganese Oxides in Water Oxidation Reactions" Angewandte, 2014, pp. 1–7.

[14]. Wu, L., Li, Q., Wu, C. H., Zhu, H., Garcia, A., Shen, B., Guo, J., Sun, S., "Stable Cobalt Nanoparticles and Their Monolayer Array as an Efficient Electrocatalyst for Oxygen Evolution Reaction," *J. Am. Chem. Soc.*, 2015, vol. 137, no. 22, pp.7071-7074.

[15]. Faid, A.Y., Barnett, A.O., Seland, F., Sunde, S., "Optimized Nickel-Cobalt and Nickel-Iron Oxide Catalysts for the Hydrogen Evolution Reaction in Alkaline Water Electrolysis," *J. Electrochem. Soc.*, 2019, vol. 166, no. 8, pp. F519–F533.

[16]. Gong, M., Dai, H., "A mini review of NiFe-based materials as highly active oxygen evolution reaction electrocatalysts," *Nano Res.*, 2014, vol. 8, no. 1, pp. 23–39.

[17]. Fominykh, K., Chernev, P., Zaharieva, I., Sicklinger, J., Stefanic, G., Doblinger, M., Muller, A., Pokharel, A., Bcoklein, S., Scheu, C., Bein, T., Rohlfing, D., "Iron-doped nickel oxide nanocrystals as highly efficient electrocatalysts for alkaline water splitting," *ACS Nano*, 2015, vol. 9, no. 5, pp. 5180–5188.

[18]. Trotochaud, L., Young, S. L., Ranney, J. K., Boettcher, S. W., "Nickel-Iron oxyhydroxide oxygen-evolution electrocatalysts: The role of intentional and incidental iron incorporation," *J. Am. Chem. Soc.*, 2014, vol. 136, no. 18, pp. 6744–6753.

[19]. Wu, G., Chen, W., Zheng, X., Hea, D., Luoa, Y., Wanga, X., Yang, J., Wu, Y., Yan, W., Zhuang, Z., Hong, X., Li, Y., "Hierarchical Fe-doped NiO_x nanotubes assembled from ultrathin nanosheets containing trivalent nickel for oxygen evolution reaction," *Nano Energy*, 2017, vol. 38, no. May, pp. 167–174.

[20]. Xiang, R., Tong, C., Wang, Y., Peng, L., Nie, Y. Li, L., Huang, X., Wei, Z., "Hierarchical coral-like FeNi(OH) x /Ni via mild corrosion of nickel as an integrated electrode for efficient overall water splitting," *Cuihua Xuebao/Chinese J. Catal.*, 2018, vol. 39, no. 11, pp. 1736–1745.

[21]. Zhang, R.,Wei, H., Si, W., Ou, G., Zhao, C., Song, M., Zhang, C., Wu, H., "Enhanced electrocatalytic activity for water splitting on NiO/Ni/carbon fiber paper," *Materials (Basel).*, 2017, vol. 10, no. 1, pp. 1–8.

[22]. Louie, M.W., Bell, A.T., "An investigation of thin-film Ni-Fe oxide catalysts for the electrochemical evolution of oxygen," *J. Am. Chem. Soc.*, 2013, vol. 135, no. 33, pp. 12329–12337.

[23]. Song, F., Busch, M. M., Kaiser, B., Hsu, C., Petkucheva, E., Bensimon, M., Chen, H. M., Corminboeuf, C., Hu, X., "An Unconventional Iron Nickel Catalyst for the Oxygen Evolution Reaction," *ACS Cent. Sci.*, 2019, vol. 5, no. 3, pp. 558–568.

[24]. Eftekhari, A., "From pseudocapacitive redox to intermediary adsorption in oxygen evolution reaction," *Mater. Today Chem.*, 2017, vol. 4, pp. 117–132.

[25]. Liu, X., Liu, W., Ko, M., Park, M., Kim, M. G., Oh, P., "Metal (Ni , Co) -Metal Oxides / Graphene Nanocomposites as Multifunctional Electrocatalysts," 2015, vol. 25, no. 36, pp. 5799–5808.

[26]. Xu, Y., Yan, Y., He, T., Zhan, K., "Supercritical CO_2 -Assisted synthesis of $NiFe_2O_4$ /vertically-aligned carbon nanotube arrays hybrid as a bifunctional electrocatalyst for efficient overall water splitting," *Carbon N. Y.*, 2019, vol. 145, pp. 201–208.

[27]. Eftekhari A., Molaei, F.,"Carbon nanotube-assisted electrodeposition. Part II : Superior pseudo-capacitive behavior of manganese oxide film electrodeposited at high current densities," *J.Power Sources*, 2015, vol. 274, pp. 1315–1321.

[28]. Ye, B., Kim, S., Lee, M., Ezazi, M., Kim, H., Kwon, G., Lee, D. H., "Synthesis of oxygen functionalized carbon nanotubes and their application for selective catalytic reduction of $NO_x$with NH_3," *RSC Adv.*, 2020, vol. 10, no. 28, pp. 16700–16708.

[29]. Gong, M., Zhou, W., Tsai, M., Zhou, J., Guan, M., Lin, M., Zhang, B., Hu, Y., Wang, D., Yang, J., Pennycook, S. J., Hwang, B., Dai, H., "Nanoscale nickel oxide/nickel heterostructures for active hydrogen evolution electrocatalysis," *Nat. Commun.*, 2014, vol. 5, pp. 1–6.

[30]. Kayani, Z. N., Saleemi, F., Batool, I., "Effect of calcination temperature on the properties of ZnO nanoparticles," *Appl. Phys. A Mater. Sci. Process.*, 2015, vol. 119, no. 2, pp. 713–720.

[31]. Shayesteh, S.F., Dizgah, A.A., "Effect of doping and annealing on the physical properties of ZnO:

Mg nanoparticles," *Pramana - J. Phys.*, 2013, vol. 81, no. 2, pp. 319–330.

[32]. Ponnusamy, P.M., Agilana, S., Muthukumarasamy, N., Senthi, T. S., Rajesha, G., Venkatramana, M. R., Velauthapillai, D., "Structural, optical and magnetic properties of undoped NiO and Fe-doped NiO nanoparticles synthesized by wet-chemical process," *Mater. Charact.*, 2016, vol. 114, pp. 166–171.

[33]. Kim, N., Sa, Y. J., Cho, S., So, I., Kwon, K., "Enhancing Activity and Stability of Cobalt Oxide Electrocatalysts for the Oxygen Evolution Reaction via Transition Metal Doping," 2016, vol.163, no. 11.

[34]. Elias, M., Aminb, M., Firozd, S. H., Hossainb, M. A., Akterb, S., Awlad Hossaina, M., Nizam Uddinb, M., Siddiquey, I. A., "Microwave-assisted synthesis of Ce-doped ZnO/CNT composite with enhanced photo-catalytic activity," *Ceram. Int.*, 2017, vol. 43, no. 1, pp. 84–91.

[35]. Jyotsna, C., Shrivastav, N., Dugaya, A., Pandey, D., "Synthesis and Characterization of Ni and Cu Doped Zno," *MOJ Polym. Sci.*, 2017, vol. 1, no. 1.

[36]. Zirak M. B., Pezeshki, A., "Effect of Surfactant Concentration on the Particle Size, Stability and Potential Zeta of Beta carotene Nano Lipid Carrier," *Int. J. Curr. Microbiol. Appl. Sci.*, 2015, vol. 4, no. 9, pp. 924–932.

[37]. Lin, C., Al-Muhtaseb, S., Ritter, J., "Thermal Treatment of Sol-Gel Derived Nickel Oxide Xerogels," Journal of Sol-gel Science and Technology, 2003, vol. 28, pp. 133-141.

[38]. Kusuma M., Chandrappa, G. T., "Effect of calcination temperature on characteristic properties of $CaMoO_4$ nanoparticles," *J. Sci. Adv. Mater. Devices*, 2019, vol. 4, no. 1, pp. 150–157.

[39]. Kwak, B., Park, S., Lee, H. S., Kim, J., Yoo, B., "Improved Chloride Ion Sensing Performance of Flexible Ag-NPs/AgCl Electrode Sensor Using Cu-BTC as an Effective Adsorption Layer," *Front. Chem.*, 2019, vol. 7, pp. 637.

[40]. Taklimi, S. R., Ghazinezami, A., Askari, D., "Chemical Functionalization of Helical Carbon Nanotubes: Influence of Sonication Time and Concentrations of Sulfuric and Nitric Acids with 3: 1 Mixing Ratio," *J. Nanomater.*, 2019, vol. 2019.

[41]. Bau, J. A., Li, P., Marenco, A. J., Trudel, S., Olsen, B. C., Luber, E. J., Buriak, J. M., "Nickel/Iron Oxide Nanocrystals with a Nonequilibrium Phase: Controlling Size, Shape, and Composition," 2014, vol. 26, no. 16, pp. 4796-48040.

[42]. Zhou, X., Yu, X. X., Kaub, T., Martens, R. L., Thompson, G. B., "Grain Boundary Specific Segregation in Nanocrystalline Fe(Cr)," *Sci. Rep.*, 2016, 6:34642.